A COMPARISON OF ABL HEIGHTS INFERRED ROUTINELY FROM LIDAR AND RADIOSONDES AT NOONTIME

(Research Note)

W. A. J. VAN PUL,[1] A. A. M. HOLTSLAG,[2] and D. P. J. SWART[1]

[1]*National Institute of Public Health and Environmental Protection (RIVM), Bilthoven, The Netherlands;*
[2]*Royal Netherlands Meteorological Institute (KNMI), de Bilt, The Netherlands*

(Received in final form 2 April, 1993)

Abstract. The height of the atmospheric boundary layer (ABL) obtained with lidar and radiosondes is compared for a data set of 43 noon (12.00 GMT) cases in 1984. The data were selected to represent the synoptic circulation types appropriately. Lidar vertical profiles at 1064 nm were used to obtain three estimates for the ABL height (h_{lid}), based on the first gradient in the back-scatter profile, namely, at the beginning, middle and top of the gradient. The boundary-layer height obtained with the radiosondes (h_s) was determined with the dry-parcel-intersection method in unstable conditions. As a first guess for near-neutral and stable conditions, the height of the first significant level in the potential temperature profile was taken.

Overall, the boundary-layer thickness estimates agree surprisingly well (regression line $h_{lidb} = h_s$: $cc. = 0.93$ and the standard error = 121 m). However, in 10% of the cases, the lidar estimate was significantly lower (difference>400 m) than the routinely inferred h_s. These outliers are discussed separately.

For stable conditions, an estimate of ABL height (h_N) is also made based on the friction velocity and the Brunt–Väisälä frequency. The agreement between h_N and h_{lidb} is good.

Discrepancies between the two methods are caused by:

(a) rapid growth of the boundary layer around the measurement time;
(b) the presence of a deep entrainment layer leading to a large zone in which quantities are not well mixed;
(c) a large systematic error of 100–200 m in the estimate of boundary-layer height obtained from the radiosonde due to the way that profiles are recorded, as a series of significant points.

1. Introduction

The height of the atmospheric boundary layer (ABL) is an important parameter in the dispersion of air pollution and its modelling (e.g., Gryning *et al.*, 1987). The height can be determined using temperature profiles from radiosondes, but these measurements are relatively sparse in time (i.e., not more than 4 times a day). Therefore, there is a need for a system to determine the ABL height more frequently.

At RIVM, a lidar has been developed which detects aerosol particles in the atmosphere. Also the height to which the aerosol particles have been mixed can be evaluated. From previous research, it was shown that lidar can determine ABL

Boundary-Layer Meteorology **68**: 173–191, 1994.

height very accurately compared with Acdar or Sodar measurements (Salemink and v.Maanen, 1985) or radiosonde data (Coulter, 1979; Boers *et al.*, 1984). These comparisons, however, were made mostly for ABLs under well defined unstable atmospheric conditions.

In this paper we compare the ABL height determined with lidar and radiosondes at about 1200 GMT for a data set extracted from an entire year (1984). The data are selected to represent the dominant weather types for the Netherlands.

2. Background

For relatively low wind speeds, the turbulent structure of an ABL is dominated by buoyancy effects. Such a strongly unstable ABL is often referred to as being convective (e.g., Holtslag and Nieuwstadt, 1986). The height of this convective boundary layer (CBL) can reach 1500–2000 m at mid-latitudes. Within the CBL, air pollutants are rather well mixed, and for this reason the CBL is often referred to as the mixing layer. At the top of the CBL, the exchange between the CBL and the layer above (the so-called reservoir layer) takes place in the entrainment layer. This region can take up the top 10 to 60% of the CBL (Stull, 1988) depending on the strength of the CBL turbulence field and the stability of the layer above. In this region, the turbulence is intermittent so no homogeneous mixing exists. In the layer adjacent to the surface, a superadiabatic lapse rate is present. A typical potential temperature profile in the CBL is shown in Figure 1a.

The height of the CBL can be found at the intersection of the adiabatic lapse rate with the actual potential temperature profile, often called the dry parcel intersection method (Holzworth, 1964). This is illustrated in Figure 1a as well. Note that with this method, the height is found up to which quantities can mix, e.g., the whole turbulent layer.

The vertical profiles of water vapour or aerosol depend on the concentration of these quantities in the reservoir layer. Inclined vertical profiles of these components are therefore often observed (Wyngaard, 1984). Especially in the entrainment zone, the quantities are not well-mixed.

Neutral stratification generally occurs on days with overcast skies and at least moderate wind speeds, with no large temperature differences between the surface and the overlying air. This means that the turbulence in the ABL is mainly driven by wind shear and is not enhanced or suppressed by stability effects.

A stable boundary layer forms when the surface is cooler than the overlying air. In such boundary layers the turbulence is mainly produced by wind shear and suppressed by the stable stratification. As a consequence, wind, temperature, air pollutants etc. show vertical gradients in the boundary layer. During daytime, such stable layers can be formed due to small surface fluxes and when warm air advection is present. In the Netherlands, this typically occurs on overcast days with advection of air transported from a relatively warm sea.

As a first approximation, the ABL height in near-neutral or stable stratification

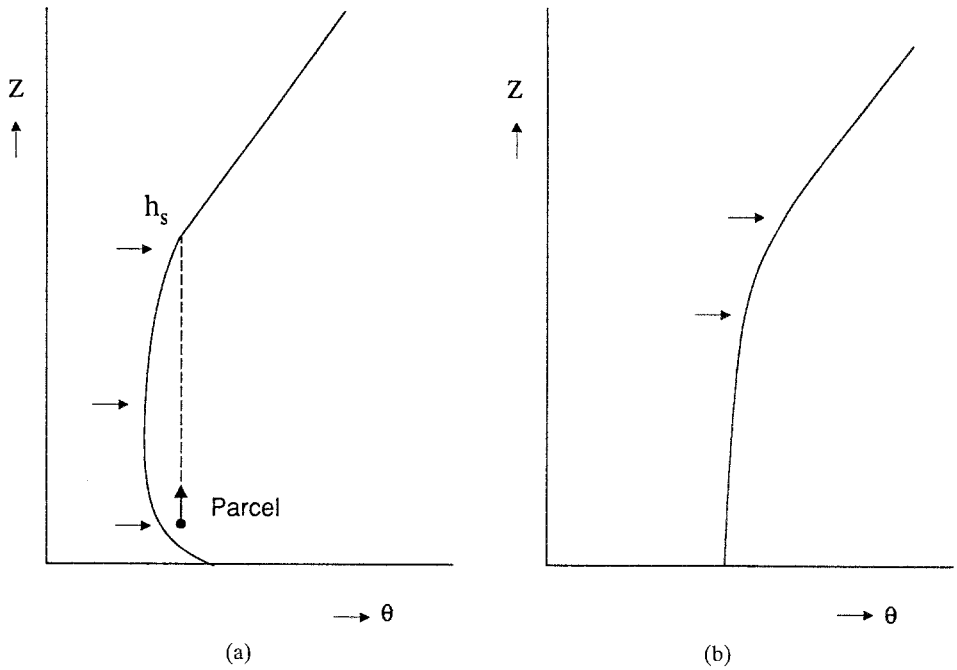

Fig. 1. Typical potential temperature profiles in the ABL during the daytime: (a) in convective conditions and (b) in near neutral or slightly stable conditions. h_s: ABL height found with the dry parcel intersection method. Significant points are indicated with arrows.

can be estimated using the first strong gradient in the temperature profile. In the radiosondes, this is indicated as a significant point in the temperature profile; see Section 3.2. Generally, this point indicates that a larger temperature inversion is present above. Generally, this approximation will give a maximum value of the ABL height. A typical potential temperature profile under slightly stable conditions is shown in Figure 1b. Under stable conditions, an estimate of the ABL height can be made with (Kitaigorodskii and Joffre, 1988):

$$h_N = c\,\frac{u_*}{N}\,. \tag{1}$$

Here c is a constant between 7–14 with a typical value of 10, u_* is the friction velocity and N the Brunt–Väisälä frequency given by:

$$N^2 = \frac{g}{T}\frac{\mathrm{d}\theta}{\mathrm{d}z}\,, \tag{2}$$

with g the acceleration due to gravity, T the absolute surface temperature and θ the potential temperature. Note that Equation (1) is limited to cases with $N > 0$.

The estimate of the ABL height by lidar is based on the detection of aerosol particles. In the reservoir layer above the ABL, the aerosol particle concentration

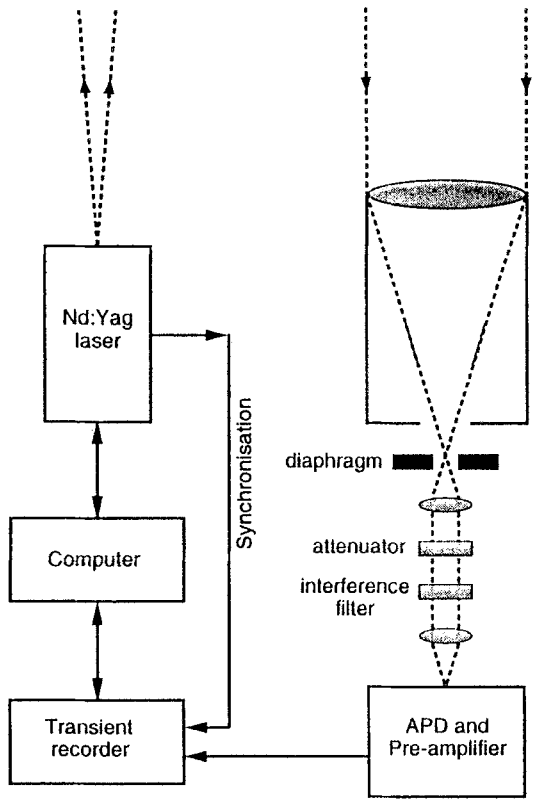

Fig. 2. Setup of the lidar system.

is considerably less. So at the top of the ABL a large gradient in aerosol particles is present. An estimate of ABL height by lidar is obtained by detecting this gradient. This method is similar under all atmospheric conditions (for details see Section 3.1).

3. Sensor and Data Description

3.1. Lidar

The lidar system used in this study is shown schematically in Figure 2. A set of relevant system and dataset parameters is given in Table I. A short, intense optical pulse is transmitted to the zenith. Molecules and especially aerosols scatter a small fraction of the light on its path through the atmosphere. The very weak optical echoes are collected by a telescope next to the transmitting laser, detected by an avalanche photodiode, and recorded and digitized as a function of time by a transient recorder. A computer performs system control, multi-echo averaging

TABLE I

Lidar system and data characteristics

Laser	Nd: Yag laser	Quanta ray type DCR 2
	Wavelength	1064 nm
	Pulse duration	9 ns
	Repetition rate	10 Hz
Telescope	Fresnel type	
	Diameter primary	0.25 m
Photodetector	Avalanche photodiode	RCA C30955E
Transient recorder	Biomation 8100	
	Sample frequency	100 Ms/s
	Resolution	8 bits
Computer	Real time minicomputer	Hewlett Packard model HP1000 A600
Dataset	Initial vertical resolution	1.5 m
	Achieved vertical resolution	50 m
	Shots averaged per profile	100
	Profile time resolution	1 profile per 10 min

and online analysis. From the strength of the echo as a function of the time elapsed since emission, a backscatter profile is calculated. Processing includes averaging of typically 100 echoes, subtraction of the optical background and correction for the geometrical decrease of intensity with range. Since beam attenuation for most situations in the ABL is negligible at the wavelength used, no attempt is made to correct for this effect.

In the ABL, aerosol particles are in general both abundant and rather well mixed, causing a high and constant backscatter in the lidar profile. The free troposphere above the ABL typically shows a considerably lower aerosol load, resulting in lower backscatter values. Consequently, the top of the ABL is associated with a negative gradient in the backscatter profile. Above the ABL, more layers can be present, which are "old" reservoir layers, with relatively high aerosol concentrations, and lead to additional gradients.

A typical example of a lidar profile of the ABL is given in Figure 3, showing an ABL with a height of about 800 m. The observed increase of the backscatter in the first 200 m is caused by incomplete overlap between transmitted beam and the field of view of the receiving telescope, an instrumental artefact.

In this study, three lidar estimates of the ABL height are made, using the first negative gradient in the backscatter profile (i.e., the gradient occurring at lowest altitude). The first value labelled "A" is defined by the onset of the gradient, a second value labelled "B" by the middle, and a third value labelled "C" by the end. The heights of the levels are indicated by h_{lida}, h_{lidb}, and h_{lidc} respectively. The three approaches are indicated in Figure 3. These values can typically be determined with an accuracy of 50 m.

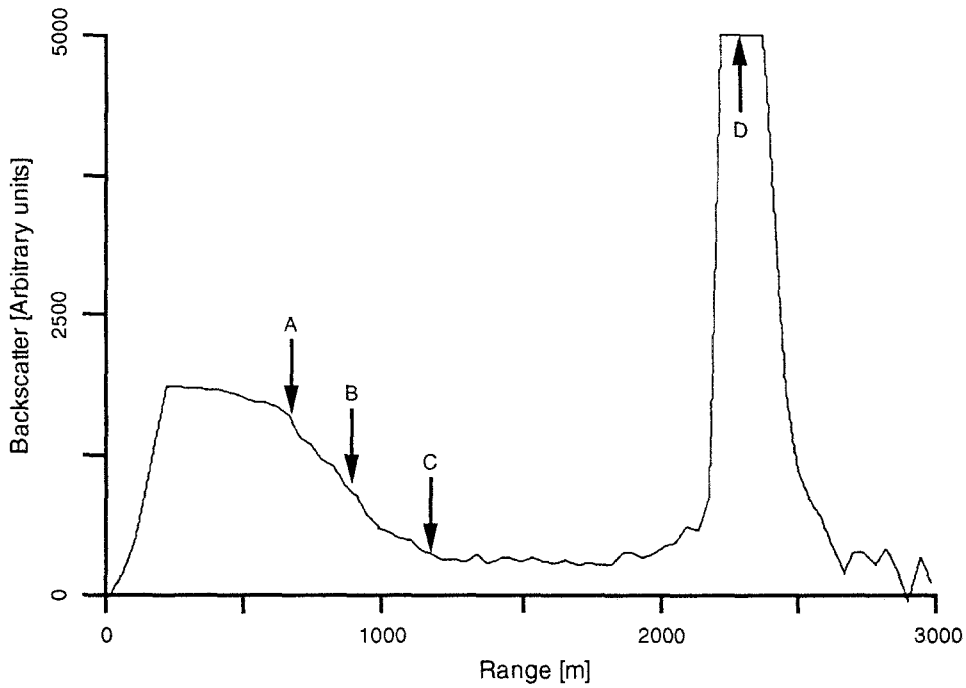

Fig. 3. Typical example of a backscatter profile measured with lidar. The top of the ABL is marked by a negative gradient (ABC). A dense cloud is observed at about 2.3 km (D). Cloud backscatter is truncated by AD-converter saturation.

3.2. Radiosondes

Radiosondes are carried out 4 times a day at de Bilt (station WMO 06260). We used the 1200 GMT sondes which are released at 11.15 GMT (to arrive at 500 mb at about 1200 GMT). The sonde equipment consisted of a Vaisala Rs-21-12C with an analog PTU recorder. The ascent rate is 5 m/s and every 10 s a signal is received from the sonde. The accuracy of the temperature measurements is typically 0.5 K. The time constant of the temperature sensor is 6 s. The error in the height of the levels is about 30 m.

The temperature profiles are plotted at significant levels in a $\theta_s - p$-diagram according to WMO standards (WMO, 1988). These levels are constructed such that the difference between the observed temperature and the temperature estimated from the linear interpolation between two significant levels is smaller than 1 K. In Figure 1a and b, the significant points deduced from two potential temperature profiles are shown. More information about this routine and the accuracy of the sondes can be obtained from Annema *et al.* (1984), Monna *et al.* (1988), and WMO (1988).

The following routine was used to determine the ABL height, h_s: when the temperature profile showed a superadiabatic lapse rate, the dry parcel intersection

method (Holzworth, 1964) was used; with a near-neutral or stable temperature profile, the height of the first significant level in the temperature profile was taken.

The way of estimating the temperature profile in the $\theta_s - p$-diagram reduces the accuracy of the temperature profiles and leads to a rough estimate of the ABL temperature profiles. The error in the estimate of the ABL height made due to this approach is about 100 m.

The accuracy of the CBL height, Δh, determined with the parcel method is estimated as: $\Delta T/\gamma$, where ΔT is the error in the temperature measurement and γ the lapse rate of the inversion above the CBL. With a value of $\gamma = 0.005$ K/m and $\Delta T \sim 0.5$ K; $\Delta h \approx 100$ m. If a temperature jump at the top of the CBL is present, this error will be smaller. The radiosondes can give only one value of the ABL height at a certain place and moment. Lidar gives the ABL height based on an average of bursts made every 10 min. The error (with regard to the ensemble average of the ABL) made by taking just one measurement lies in the order of 100 m for the CBL height (Driedonks, 1981). In the morning hours, the ABL height can rise very rapidly, i.e., typically 0.1 m/s. Due to the spatial difference of 2 km between the two observation sites and the possible time shift between the measurements, a difference between the two determinations of ABL height is introduced. This difference will be typically in the order of 100 m.

Under the assumption that all the above errors are randomly distributed, the total inaccuracy is estimated at 170 m.

For the stable cases, an additional estimate of ABL height was made with Equation (1). The friction velocity was calculated from the 10 m wind speed observed at Soesterberg, which is 8 km from de Bilt. Using the local roughness, this 10 m wind speed, permitted us to estimate a wind at 60 m. For this, a mesoscale friction velocity was calculated according to a mesoscale roughness representative for a larger area (typically 10 km) (Wieringa, 1986). Since the profiles were categorized as near neutral or slightly stable, the calculations were made without stability corrections. The potential temperature gradient was deduced from the radiosonde launchings. For a number of cases ($n = 6$), the h_N could not be estimated due to a very small potential temperature gradient ($\gamma < 0.001$ K/m). These cases were excluded from this sub-dataset.

3.3. Description of the data set

In the present study, 43 days were selected from the radiosonde releases of 1200 GMT in 1984. This selection was carried out using a climatology of synoptic circulation types known as "GrossWetterLagen" (GWL, Hess and Brezowsky, 1977) from 1949–1980. The days were selected according to their frequency of occurrence in this GWL climatology. In Table II the data set is partitioned into a summer and winter period and into unstable and neutral/stable atmospheric conditions during the daytime. The cloud covers for the data set are: $N \leqslant 3$, $n = 21$ and $N > 3$, $n = 22$.

TABLE II

Number of data points in summer and winter periods and unstable and near-neutral stable atmospheric conditions

	Summer	Winter	Total
Unstable "*u*"	15	12	27
Neutral/stable "*s*"	4	12	16
Total	19	24	43

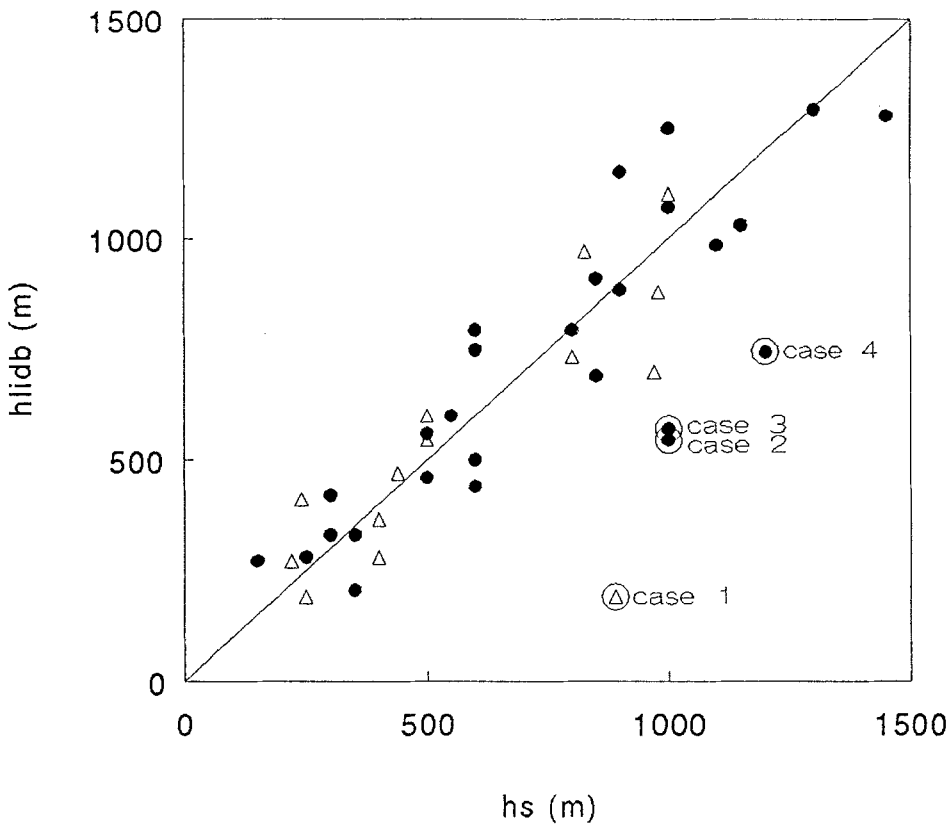

Fig. 4 Comparison of ABL heights at 1200 GMT detected with radiosondes (h_s) and lidar (h_{lidb}) for 43 days, 1984. Unstable cases are indicated with dots and neutral or slightly stable cases with triangles. Also the 1:1 line and the cases for which $h_s - h_{lidb} > 400$ m are presented.

4. Results and Discussion

4.1. General results

A comparison of values of h_s and h_{lidb} for the total data set is depicted in Figure 4. It can be inferred from this figure that apart from four outliers, the correlation

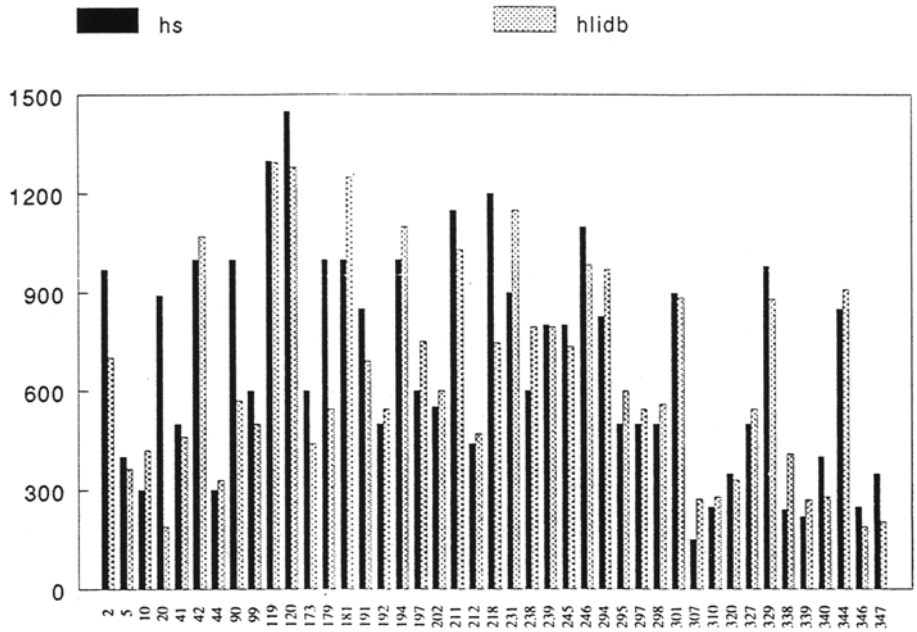

Fig. 5. The height of the ABL detected by radiosonde (h_s) and lidar (h_{lidb}) for 43 days in 1984.

between the two heights was good. The outliers are eliminated from the data set in the regression analysis and are discussed in the next section.

The course of the ABL height (h_s and h_{lidb}) throughout the year is given in Figure 5. The average height of the ABL was 688 and 650 m and ranged between 150–1450 m and 190–1295 m for h_s and h_{lidb} respectively.

Linear regression lines and the statistics of this regression are presented in Table III. h_{lida} was 17% smaller than h_s. h_{lidb} and h_{lidc} were respectively slightly smaller and larger than h_s. This indicated that both the b and c values may be used to detect the ABL height. However, the detection of ABL height with h_{lidc} could only be used in 80% of the cases. This suggests that h_{lidb} is the most reliable estimator of ABL height. Salemink and van Maanen (1985) found that the b spot in the gradient correlated well with Acdar measurements. The b spot in the gradient is better defined than the beginning or end of this gradient. The "a" spot underestimates the ABL height especially in the case of weak gradients (large entrainment zones).

The standard error of the regression ($h_s = h_{lidb}$) is 121 m, i.e., 20% of the ABL height. From Figure 4 it can be seen that the deviation is largely constant over the entire range of the measurements. This indicates an inaccuracy of both methods of about 100–200 m and is an absolute error such as readoff error from the $\theta_s - p$ diagrams.

TABLE III

Regression analysis of comparisons between the boundary-layer heights inferred from sondes (h_s) and lidar ($h_{lida,b,c}$) for various subsets and those calculated with Equation (1), h_N and $h_{N'}$, for the best regression line, $y = ax + b$, and the regression line through the origin, $y = cx$. Column 1 shows the variables used in the regression: column 2, the number of cases: columns 3, 4, 5 and 6, the slope (a), the intercept (b), the standard error in estimated y value and the regression coefficient of the regression $y = ax + b$ respectively: 7, 8 and 9 the slope c, the standard error in estimated y value and the correlation coefficient of the regression $y = cx$.

x	y	n	a	b	y est std. err.	cc	c	y est std. err	cc
h_s	h_{lidb}	39	0.92	64	119	0.93	1.00	121	0.93
h_s	h_{lida}	31	0.83	7	144	0.89	0.83	141	0.93
h_s	h_{lidc}	32	0.97	139	133	0.93	1.14	147	0.91
h_s	h_{lidb}								
Subsets:									
Unstable	Cases	24	0.93	66	127	0.93	1.00	127	0.93
Stable	Cases	15	0.88	76	114	0.91	0.99	115	0.90
$N_c \leq 3$		19	0.80	129	93	0.96	0.95	114	0.94
$N_c > 3$		20	1.15	−85	122	0.93	1.04	123	0.93
h_N	h_{lidb}	10	0.44	144	142	0.81	0.62	156	0.74
$h_{N'}$	h_{lidb}	10	0.82	3	131	0.85	0.83	123	0.85

No systematic differences were found between h_s and h_{lidb} for the stable and unstable cases. This indicates that the usage of the first significant point in the temperature profile is a rather good estimator of ABL height. The mean of the ABL height in all neutral/stable cases was 568 m. Generally the nocturnal stable ABL height is much smaller than this value (Nieuwstadt, 1981; Stull, 1988). So mainly this category existed of near-neutral or slightly stable cases which generally have larger ABL heights. The mean unstable ABL height was 746 m.

To observe the influence of clouds, the subsets with $N_c \leq 3$ and $N_c > 3$ were examined. No large differences were found between the two data sets. This indicated that the detection of ABL height by lidar was not severely hindered by clouds.

From Table III it can be inferred that h_N provides a reasonably good estimate for h_{lidb} is stable cases; but with $c = 10$ in Equation (1), h_{lidb} is overestimated by about 60%. This indicates that our data perform best with $c = 6$ in Equation (1).

An approximation of Equation (1), h'_N, can be made by using an average temperature gradient in the ABL. For this data set, this is $4 \cdot 10^{-3}$ K/m. This leads to an approximation of Equation (1); $h'_N = 840u_*$. For this data set, the linear correlation between h'_N and h_{lidb} is rather good but leads to an overestimate of h_{lidb} with 20%. Here our data perform best with $c = 8$ in Equation (1).

4.2. Case studies

In this section four cases are briefly discussed in which the discrepancies between the two methods were much larger than the standard error in the regression of h_s

and h_{lidb} (121 m). In these case studies, h_{lidb} is taken as the ABL height detected by lidar.

For these four cases, the ABL height was also calculated using a simple entrainment relation by van Dop *et al.* (1982) based on a mixed-layer model by Tennekes (1973) (see Appendix). In this equation the growth of the mixed layer caused by mechanical (wind shear) and thermal (convection) turbulence is modelled. The inputs required for this equation are the surface fluxes and the thermal stability (temperature gradient) of the upper layer. The surface fluxes were calculated with the flux library of Beljaars and Holtslag (1990), using synoptic weather data from de Bilt from 0600–1200 GMT (see Holtslag and van Ulden, 1983 for details). Except for Case 1, the ABL was unstable during this period. The temperature gradient of the upper layer was deduced from radiosondes at 0000 and 1200 GMT. Since this relation gives the growth rate of the ABL, an initial value has to be assumed. Here we used a value of 100 m at 0600 GMT or when the ABL became unstable after that time. The model is rather insensitive to this initial value. From then on, the surface fluxes and the ABL height were calculated every hour until 1200 GMT. The accurracy of the calculated values depends on the temperature profiles and is discussed per case. The cloud base is derived from the synoptic data.

Case 1

This case represents day #20 (January 20, 1984) for which h_s = 890 m and h_{lidb} = 190 m. Temperature and humidity profiles of the radiosonde launching and backscatter plot of a lidar shot are presented in Figure 6a and b, respectively. The stability of the ABL changed from stable to unstable at about 0900 GMT. During the period from 0000 to 1000 GMT the wind was very weak (<1 m s^{-1}). From 1000 to 1200 GMT the wind was about 2–3 m s^{-1}. The sensible heat flux was very small (<30 W m^{-2}) and was insufficient to clear the morning inversion. The ABL height was calculated to be 150 m using the entrainment equation. A sensitivity test yielded a maximum ABL of 500 m when the lapse rate of the upper layer was decreased towards its 1200 GMT value. Using Equation (1), we obtain h_N = 550 m.

The temperature profile was stable in the lowest 900 m (first significant point) and no significant point in this layer was found, so the ABL height was taken as this height by definition. At 200 m, a significant point in the dew point temperature was present. The height of the base of some Cumulus clouds (1 octa) was observed between 600–1000 m. The lidar observed two layers at 190 and 920 m. The height of the first layer is taken as the ABL height by definition. The second layer is probably associated with the cloud base. In this case it is very unlikely that the height of the ABL reached 900 m given the stability of the lower air layer. It is possible that the radiosonde did not detect a small temperature gradient near the ground at the same height as the dew point gradient. We conclude that in this case the first significant point very likely overestimated the actual ABL height and also that the radiosonde estimate (h_N = 550 m) is probably too large.

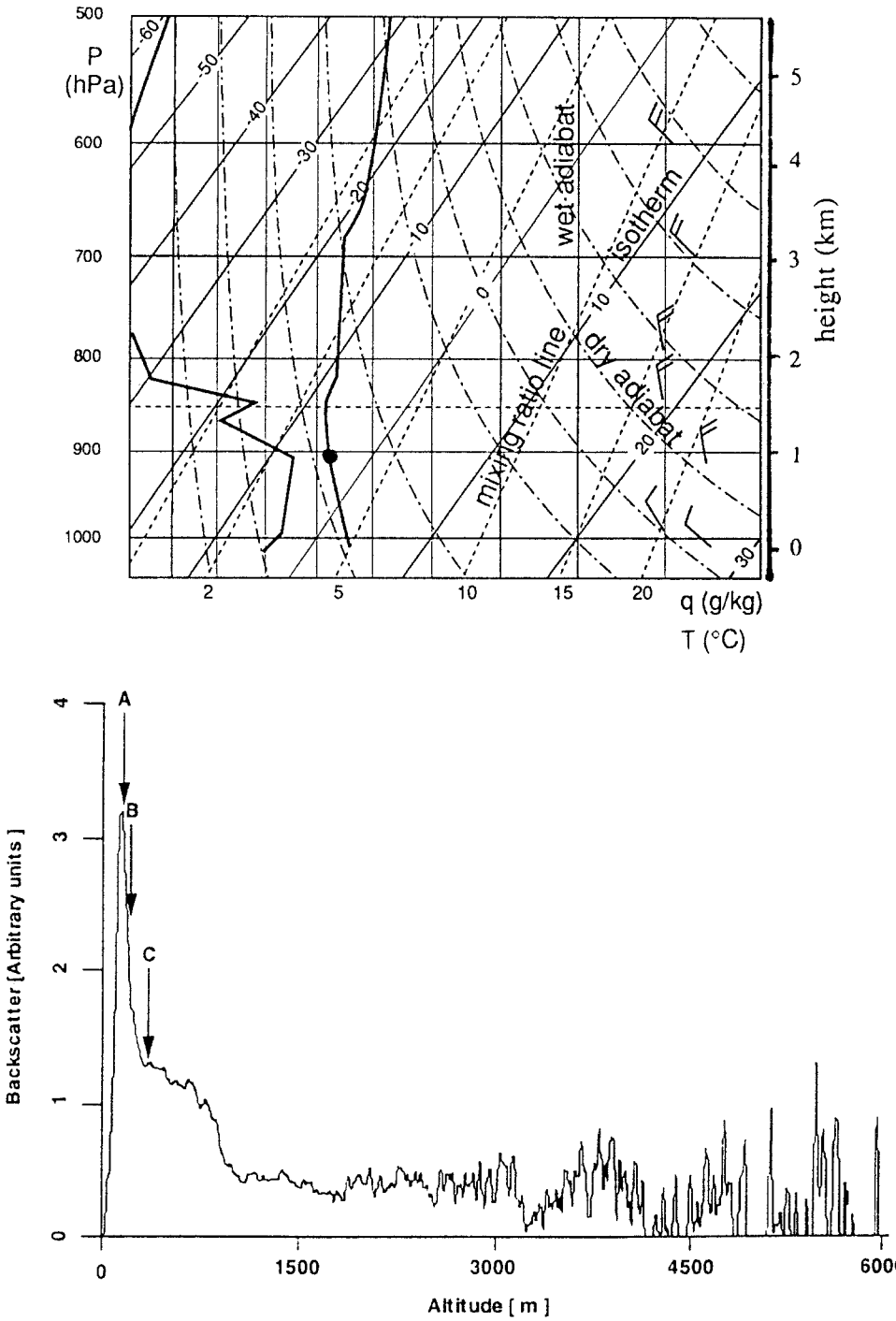

Fig. 6. Temperature (a) and humidity (b) profiles of the radiosonde and backscatter plot of a lidar shot of January 20, 1984 (day #20, case 1). h_s = 890 m, h_{lidb} = 190 m. h_s is indicated with a black dot. The arrows indicate the A, B and C spot in the first backscatter gradient.

Case 2

This case represents day #90 (March 30, 1984) for which $h_s = 1000$ m and $h_{lidb} = 570$ m. Temperature and humidity profiles of the radiosonde launching and backscatter plot of a lidar shot are presented in Figure 7a and b, respectively. The sensible heat flux had a maximum of about 90 W m^{-2} at noon. Starting with a very strong inversion ($\gamma \approx 0.02$ K m^{-1}) up to 200 m, the ABL height was calculated at about 900 m at 1200 GMT. Sensitivity studies showed that this is a conservative value.

The temperature profile followed a dry adiabatic lapse rate up to the first significant point at 1000 m. Also a significant point in the dew point temperature profile was present at 1000 m. This indicated a warmer and drier air layer above 1000 m. The air above 1000 m was weakly stable ($\gamma \approx 0.002$ K m^{-1}) so a deep entrainment layer was present. The base of some cumulus clouds (4 octas) did occur between 600–1000 m.

The lidar echo was very small over the full range, indicating a very clean atmosphere. A very weak gradient was observed in the region of 400 to 800 m. Interpretation of the profile in terms of ABL height is difficult. Lidar measurements and model calculations showed a growth of the ABL height at 1200 GMT of about 200 m per hour.

In this case, it is more likely that the ABL height was about 1000 m. The rapid development of the ABL height at sampling time and the large variations of the ABL height due to a deep entrainment layer, probably caused the difference of about 400 m between the two methods. We conclude that in this case the ABL height was not very well defined (a deep entrainment zone was present) and the lidar measurement was not reliable.

Case 3

This case represents day #179 (June 27, 1984) for which $h_s = 1000$ m and $h_{lidb} = 545$ m. Temperature and humidity profiles of the radiosonde launching and backscatter plot of a lidar shot are presented in Figure 8a and b respectively.

The sensible heat flux had a maximum of 110 W m^{-2} at 1000 GMT. In the initial profile a strong nocturnal inversion was present up to 400 m. The ABL height was calculated at 850 m.

The temperature profile was unstable up to 1000 m and was very irregular which indicated that different layers were present. In the analysis with the parcel method the height of the CBL was found at 1000 m though a stable layer from 500–1000 m was present. A dense Cumulus cloud cover (7 octas) was present with a base between 600–1000 m.

The lidar detected a pronounced cloud layer with a base at 1000 m. Below this layer a clear and steep gradient was observed between 515 and 600 m.

We conclude that both sonde and lidar show a layered structure with significant points at 500 and 1000 m. This may have been caused by advection. Given the

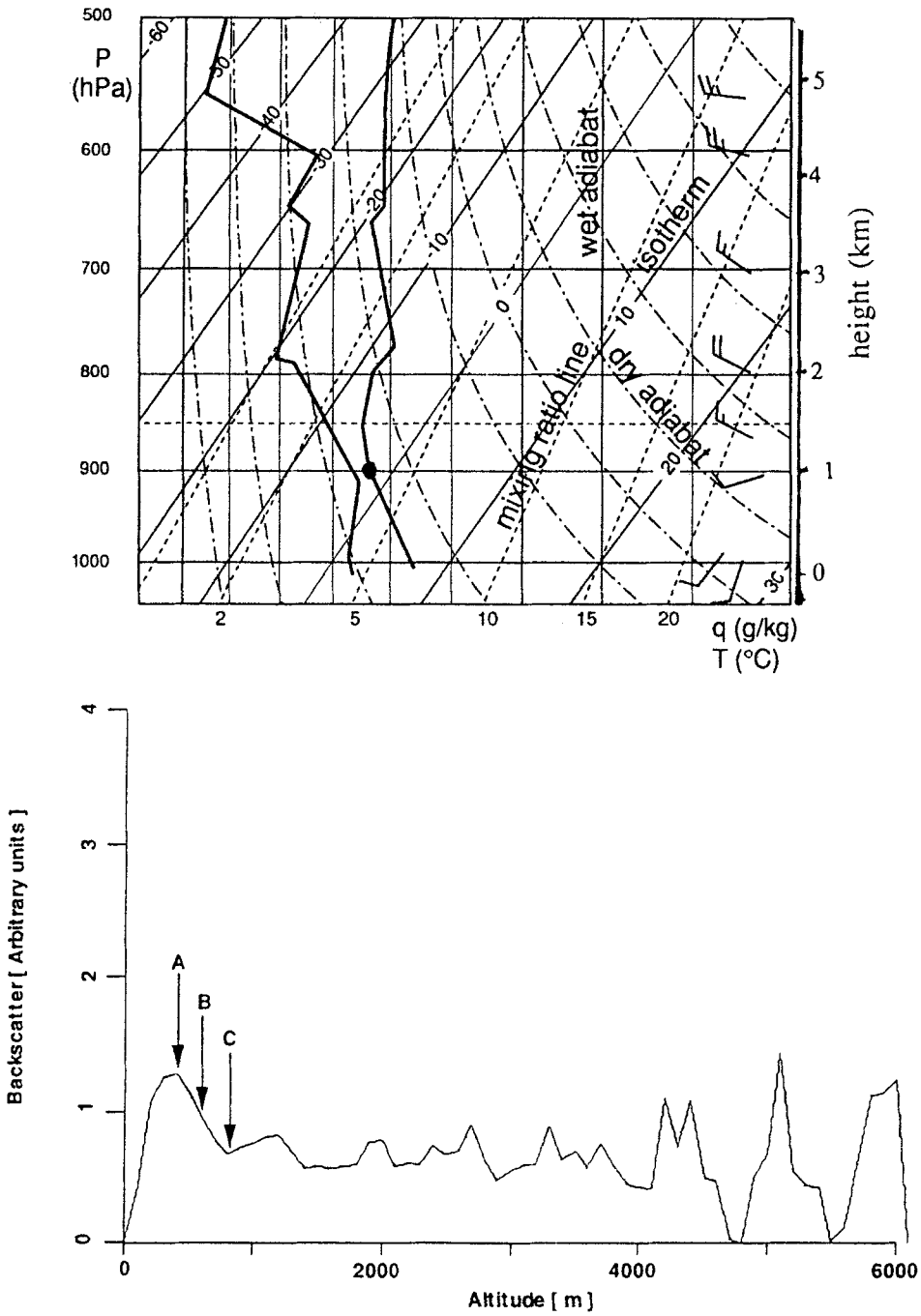

Fig. 7. Temperature (a) and humidity (b) profiles of the radiosonde (upper) and backscatter plot of a lidar shot of March 30, 1984 (day #90, case 2) (lower). $h_s = 1000$ m, $h_{lidb} = 570$ m. h_s is indicated with a black dot. The arrows indicate the A, B and C spot in the first backscatter gradient.

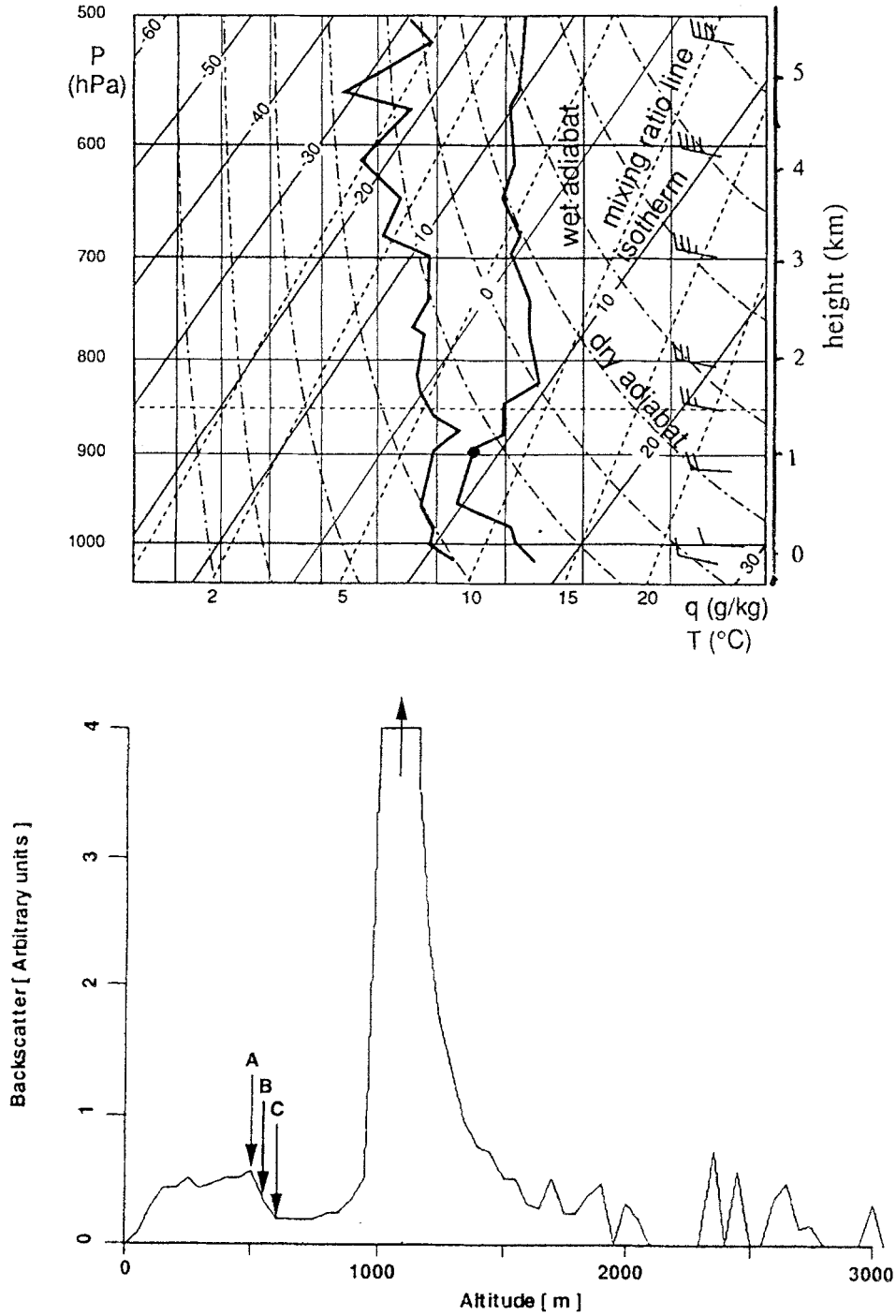

Fig. 8. Temperature (a) and humidity (b) profiles of the radiosonde (upper) and backscatter plot of a lidar shot of June 27, 1984 (day #179, case 3) (lower). $h_s = 1000$ m, $h_{lidb} = 545$ m. h_s is indicated with a black dot. The arrows indicate the A, B and C spot in the first backscatter gradient.

large instabilities of the layer up to 1000 m, it is more likely that a quantity can mix up to 1000 m. However, this mixing is intermittent and will not result in a well-mixed layer for all quantities up to 1000 m. This can lead to a different determination of the CBL height by the two methods.

Case 4

This case represents day #218 (August 5, 1984) for which $h_s = 1200$ m and $h_{lidb} = 745$ m. Temperature and humidity profiles of the radiosonde launching and back-scatter plot of a lidar shot are presented in Figure 9a and b, respectively.

The sensible heat flux had a maximum of about 80 W m^{-2} at noon. With the entrainment relation, an ABL height of about 840 m was calculated. The temperature profile was slightly superadiabatic up to 1000 m. Boundary-layer clouds (3 octa's) were present with a base at 600–1000 m. The air layer above the CBL was weakly stable ($\gamma \approx 0.003$ K m^{-1}) so a deep entrainment layer was present.

An estimate of the depth of this layer is given by the difference between the first significant point at 900 m in the temperature profile and h_s, i.e., about 300 m. The lidar showed a gradient at 750 m.

Due to this deep entrainment layer, a large discrepancy between the two methods existed. We conclude that as in the previous case, the ABL height was not well defined.

5. Conclusions

In this study we compared estimates of boundary-layer height obtained from radiosonde and lidar measurements around noontime (1200 GMT). The estimates of boundary-layer height with radiosonde, h_s, were carried out using the dry-parcel-intersection method in unstable conditions and the first significant point in the temperature profile in near-neutral or stable cases. The estimate of boundary-layer height with lidar, h_{lid}, was made using the first gradient in the back-scattered signal nearest the surface. The beginning, middle and end of the gradient were used to define three estimates namely: h_{lida}, h_{lidb} and h_{lidc}.

Overall, the boundary-layer thickness estimates of lidar and radiosondes agree surprisingly well (regression line $h_{lidb} = h_s$: *cc.* = 0.93 and standard error = 121 m). However, in 10% of the present cases the lidar estimate was significantly lower (difference > 400 m) than the routinely inferred h_s.

Discrepancies between the two methods are caused by:

(a) a rapid growth of the ABL around the measurement time,
(b) the presence of a deep entrainment layer leading to a large zone in which quantities are not well mixed,
(c) a large systematic error of 100–200 m in h_s introduced by the representation of the profiles by significant points.

Lidar ABL height measurements h_{lidb} and h_{lidc} compared equally well with the

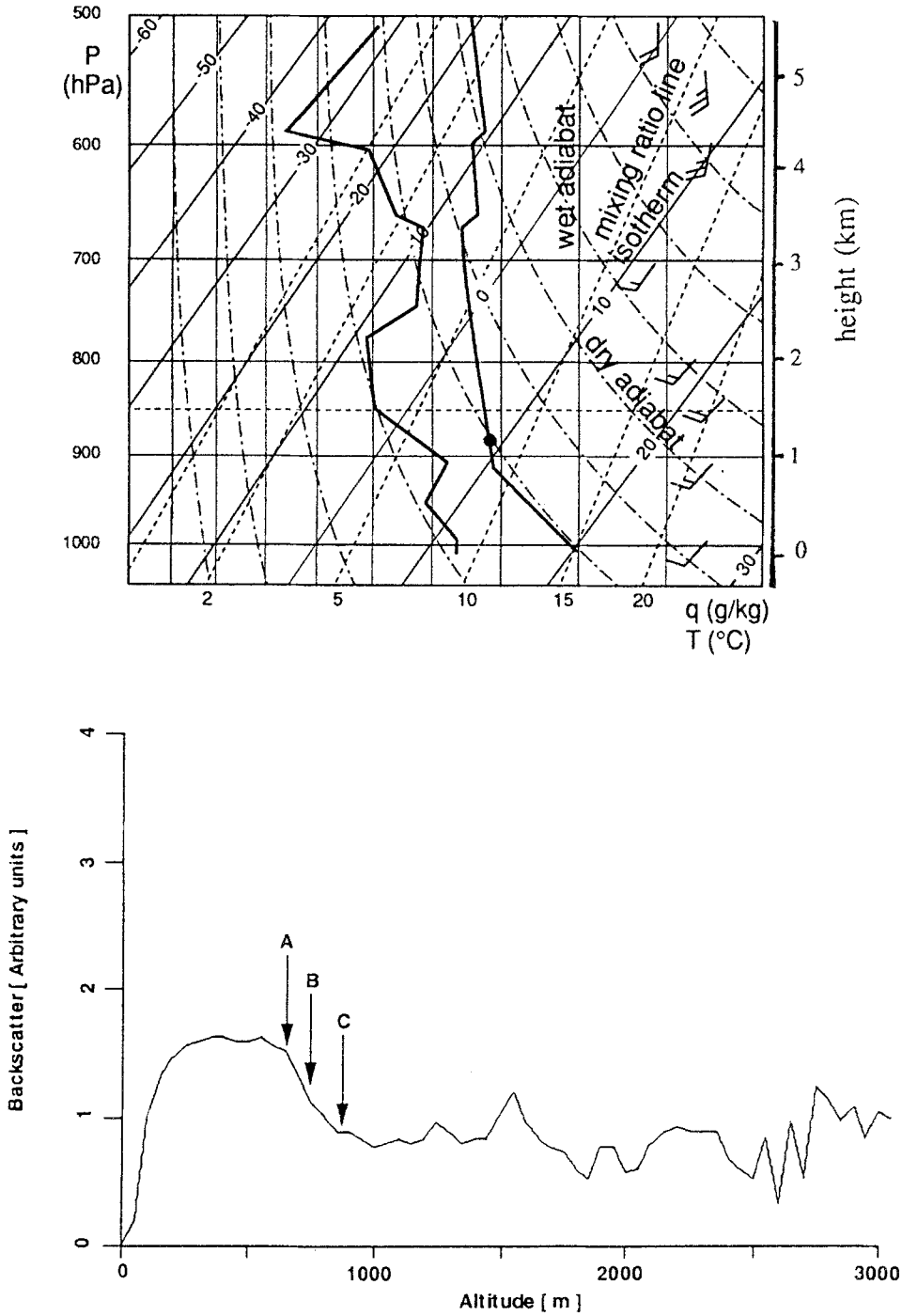

Fig. 9. Temperature (a) and humidity (b) profiles of the radiosonde (upper) and backscatter plot of a lidar shot of August 5, 1984 (day #218, case 4) (lower). $h_s = 1200$ m, $h_{lidb} = 745$ m. h_s is indicated with a black dot. The arrows indicate the A, B and C spot in the first backscatter gradient.

radiosonde measurements. However, h_{lidb} can be determined from the profile more often than h_{lidc}. No systematic differences were found between h_s and h_{lidb} between near-neutral/stable and unstable cases. This indicates that the detection of h_s using the first significant point in the temperature profile in near-neutral and stable atmospheric conditions is a reasonable good estimate.

Generally the influence of cloud cover was small on the performance of both methods. In stable conditions, an estimate of the ABL height (h_N) based on the friction velocity and the Brunt–Väisälä frequency was also made. The agreement between h_N and h_{lidb} is good but leads to an overestimate of h_{lidb} by h_N. Our data perform best with a value of 6–8 for the coefficient c in Equation (1).

Acknowledgements

We thank Mr. J. B. Bergwerff for making the lidar data available and for his help in interpreting the data. We also thank Dr F. A. A. M. de Leeuw and Dr. E. Visser for their comments on previous versions of the manuscript.

Appendix: Equation for the Entrainment rate in the CBL

The entrainment rate or the growth of the ABL height h, under convective circumstances can be approximated with (van Dop *et al.*, 1982):

$$\frac{\mathrm{d}h}{\mathrm{d}t} = \frac{F_s\left(1 + 2c_1 + \dfrac{2\kappa^2 c_2^2}{c_1}\left(\dfrac{L}{h}\right)^2\right)}{\gamma h\left(1 - \dfrac{\kappa c_2}{c_1}\dfrac{L}{h}\right)}, \tag{1}$$

where κ is 0.41, c_1 is 0.2, c_2 is 5. F_s in the sensible heat flux in $\mathrm{mK\,s^{-1}}$, and L is the Obukhov length.

References

Annema, K. H., Monna, W. A. A. and Muller, S. H.: 1984, 'A Comparative Investigation of Three Commercial Radiosonde Systems', in: *Instruments and Observing Methods Report No. 15:* WMO Technical Conference on Instruments and Cost-Effective Meteorological Observations (TECEMO), Noordwijkerhout, The Netherlands, pp. 24–27.

Beljaars, A. C. M. and Holtslag, A. A. M.: 1990, 'Description of a Software Library for the Calculation of Surface Fluxes', *Environmental Software* **5**, 60–68.

Boers, R., Eloranta, E. W. and Coulter, R. L.: 1984, 'Lidar Observations of Mixed-Layer Dynamics: Tests of Parameterized Entrainment Models of Mixed-Layer Growth Rate', *J. Climate Appl. Meteorol.* **23**, 247–266.

Coulter, R. L.: 1979, 'A Comparison of Three Methods for Measuring Mixing-Layer Height', *J. Appl. Meteorol.* **18**, 1495–1499.

Dop, H. van, de Haan, B. J. and Engeldal, C.: 1982, 'The KNMI Mesoscale Air Pollution Model', Scientific Report 82–6, Royal Netherlands Meteorological Institute, De Bilt.

Driedonks, A. G. M.: 1981, 'Dynamics of the Well-Mixed Atmospheric Boundary Layer', Scientific Report 81–2, Royal Netherlands Meteorological Institute, De Bilt.

Gryning, S. E., Holtslag, A. M. M., Irwin, J. S. and Sivertsen, B.: 1987, 'Applied Dispersion Modelling Based on Meteorological Scaling Parameters', *Atmos. Environ.* **21**, 79–89.

Hess, P. and Brezowsky, H.: 1977, 'Katalog der Grosswetterlagen Europa's. 3., verbesserte und ergänzte Auflage', Berichte des Deutchen Wetterdienstes, p. 113.

Holtslag, A. A. M. and Nieuwstadt, F. T. M.: 1986, 'Scaling the Atmospheric Boundary Layer', *Boundary-Layer Meteorol.* **36**, 201–209.

Holtslag, A. A. M. and van Ulden, A. P.: 1983 'A Simple Scheme for Daytime Estimates of the Surface Fluxes from Routine Weather Data', *J. Climate Appl. Meteorol.* **22**, 517–529.

Holzworth, G. C.: 1964, 'Estimates of Mean Maximum Mixing Depths in the Contiguous United States', *Monthly Weather Review* **92**, 235–242.

Kitaigorodskii, S. A. and Joffre, S. M.: 1988, 'In Search of a Simple Scaling for the Height of the Stratified Atmospheric Boundary Layer', *Tellus* **40A**, 419–433.

Monna, W. A. A. and Annema, K. H.: 1988, 'A Comparative Investigation of the Vaisala Microcora and Digicora Ground Systems', in: *Instruments and Observing Methods Report No. 33:* WMO Technical Conference on Instruments and Cost-Effective Meteorological Observations (TECEMO), Noordwijkerhout, The Netherlands, 24–27 September 1984.

Nieuwstadt, F. T. M.: 1981, 'The Nocturnal Boundary Layer', Theory and Experiments. Scientific Report 81-1, Royal Netherlands Meteorological Institute, De Bilt.

Salemink, H. W. M. and van Maanen, E. A.: 1985, Toepassingen van de LIDAR-meettechniek in atmosferisch onderzoek. RIVM rapport: 228201006 (in Dutch).

Stull, R. B.: 1988, *An Introduction to Boundary Layer Meteorology*, Deventer: Kluwer Academic Publishers,

Tennekes, H.: 1973, 'A Model for the Dynamics of the Inversion above a Convective Boundary Layer', *J. Atm. Sci.* **30**, 558–567.

Wieringa, J.: 1986, 'Roughness-Dependent Geographical Interpolation of Surface Wind Speed Averages', *Quart. J. Royal Meteorol. Soc.* **112**, 867–889.

WMO, 1988, International Codes, Volume I (Annex II to WMO Technical Regulations), WMO No. 306, WMO Geneva, Switzerland.

Wyngaard, J. C.: 1984, 'Toward Convective Boundary Layer Parameterization: A Scalar Transport Module', *J. Atm. Sci.* **41**, 1959–1969.